

# Efficient Pd<sup>0</sup>-Catalyzed Asymmetric Activation of Primary and Secondary C–H Bonds Enabled by Modular Binapine Ligands and Carbonate Bases

Philipp M. Holstein,<sup>†</sup> Maria Vogler,<sup>†</sup> Paolo Larini,<sup>†</sup> Guillaume Pilet,<sup>§</sup> Eric Clot,<sup>\*,‡</sup> and Olivier Baudoin<sup>\*,†</sup>

<sup>†</sup>Université Claude Bernard Lyon 1, CNRS UMR 5246 – Institut de Chimie et Biochimie Moléculaires et Supramoléculaires, CPE Lyon, 43 Boulevard du 11 Novembre 1918, 69622 Villeurbanne, France

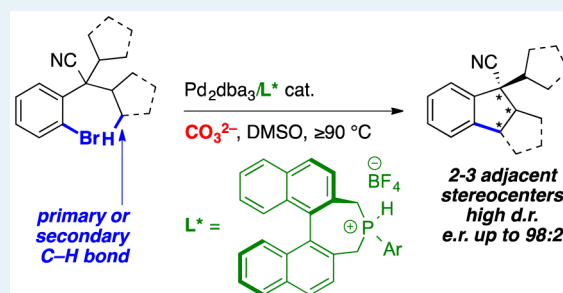
<sup>§</sup>Université de Lyon, Laboratoire des Multimatériaux et Interfaces, UMR 5615 CNRS - Université Claude Bernard Lyon 1, Campus de la Doua, Avenue du 11 Novembre 1918, 69622 Villeurbanne, France

<sup>‡</sup>Institut Charles Gerhardt, CNRS UMR 5253, Université Montpellier, case courrier 1501, Place Eugène Bataillon, 34095 Montpellier, France

## Supporting Information

**ABSTRACT:** New binapine ligands have been synthesized, and characterized and have been shown to induce high diastereo- and enantioselectivity in the intramolecular arylation of primary and secondary C(sp<sup>3</sup>)–H bonds, giving rise to fused cyclopentanes. The ligands were obtained as bench-stable phosphonium tetrafluoroborate salts that can be directly employed in catalysis. It was shown that a ferrocenyl P-substituent on the ligand allows achievement of high stereoselectivities in combination with potassium carbonate for the arylation of primary C–H bonds under unprecedentedly low temperature (90 °C) and catalyst loading (1–2 mol % Pd/2–3 mol % ligand). Using a base-free precatalyst, carbonate was shown to be the active base and to provide higher stereoselectivities than acetate and pivalate. The more difficult arylation of secondary C–H bonds could also be achieved and required fine-tuning of the ligand structure and the carbonate counteranion. This method allowed generation of fused tricyclic products containing three adjacent stereocenters as single diastereoisomers and with moderate to high enantioselectivity. Experimental data indicated that the enantiodetermining C–H activation step involves a monoligated species. DFT (PBE0-D3) calculations were performed with a prototypical binapine ligand to understand the origin of the enantioselectivity. The preference for the major enantiomer was traced to the establishment of a more efficient network of weak attractive interactions between the phosphine ligand and the substrate.

**KEYWORDS:** asymmetric catalysis, C–C coupling, C–H activation, chiral phosphines, palladium



## INTRODUCTION

Transition-metal catalysis has recently emerged as a powerful tool to functionalize otherwise unreactive C(sp<sup>3</sup>)–H bonds.<sup>1</sup> In this context, our group<sup>2</sup> as well as others<sup>3</sup> have synthesized a diverse array of fused carbocycles and heterocycles by intramolecular palladium(0)-catalyzed arylation of unactivated C(sp<sup>3</sup>)–H bonds from aryl halides. Recent efforts have been directed toward the development of asymmetric versions of these reactions. In particular, the groups of Kündig, Kagan, and Cramer reported the synthesis of (fused) indolines (Scheme 1a) with high enantioselectivity through the activation of methyl or methylene C–H bonds using chiral N-heterocyclic carbene (L<sup>1</sup>) or phosphine (L<sup>2</sup>–L<sup>3</sup>) ligands.<sup>4</sup> Shortly thereafter, Cramer and co-workers described the enantioselective arylation of cyclopropane C–H bonds in related nitrogenated systems using chiral phosphoramidites (L<sup>4</sup>, Scheme 1b).<sup>5</sup> In parallel, we communicated our initial findings on the diastereo- and enantioselective synthesis of fused cyclopentanes via asymmetric C–H activation employing binapine-type ligand 1a

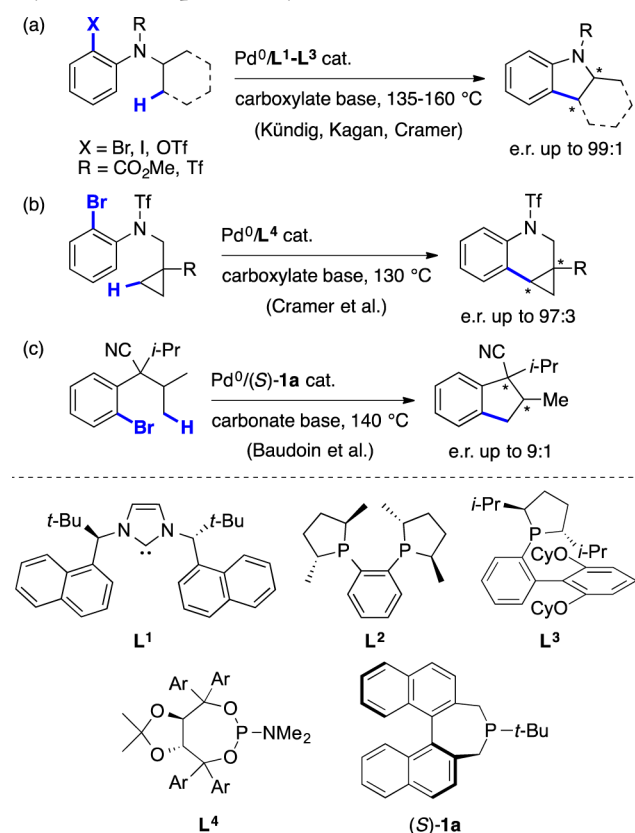
(Scheme 1c).<sup>6</sup> High diastereoselectivities, albeit moderate enantioselectivities (e.r. 76:24–90:10), were achieved.

Several observations can be made from these literature precedents. First, different classes of ligands seem to be required to achieve optimal enantioselectivities for various classes of substrates (a–c). This indicates a strong substrate dependency of this asymmetric reaction and suggests the necessity to develop highly modular ligands to achieve broad substrate scope. Second, the activity of the developed catalytic systems clearly shows room for improvement, since little reaction was observed at temperatures below ~120 °C.<sup>4</sup> However, high enantioselectivities were achieved despite the employed high temperatures (130–160 °C), showing that the developed chiral catalysts are robust and suggesting that these reactions have negligible entropy variations. In this full account,

Received: April 30, 2015

Revised: May 31, 2015

Published: June 4, 2015

Scheme 1. State-of-the-Art of Pd<sup>0</sup>-Catalyzed Intramolecular Asymmetric C(sp<sup>3</sup>)-H Arylation

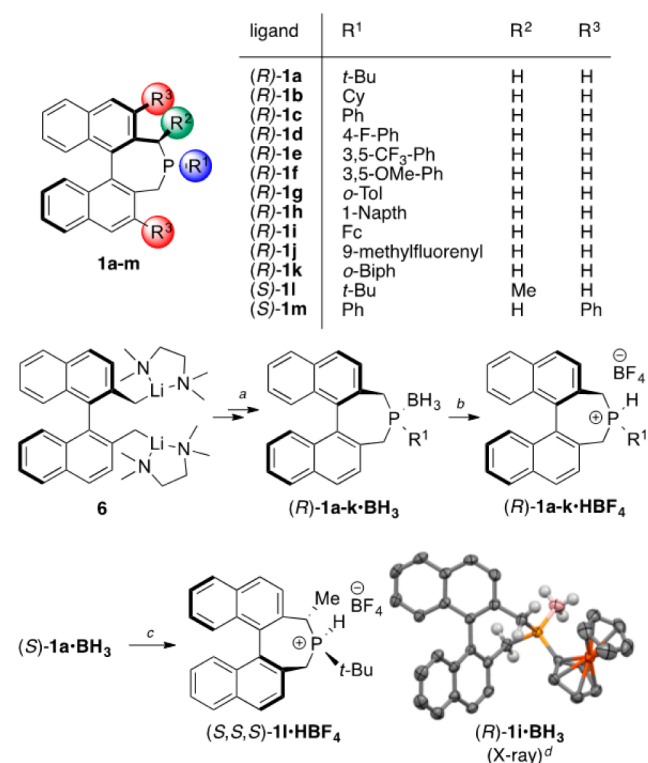
we report major improvements of both the enantioselectivity and the catalyst efficiency in the activation of primary C–H bonds giving rise to fused cyclopentanes, through the synthesis of second-generation binerine ligands combined to carbonate bases. In addition, the scope of the reaction was extended to the rarer and more challenging activation of methylene C–H bonds.

## SYNTHESIS AND PROPERTIES OF NEW BINERINE LIGANDS

Binerines are versatile chiral monodentate ligands that have found applications in a variety of asymmetric transformations.<sup>7</sup> They are readily available from BINOL and can be readily modified at the R<sup>1</sup>, R<sup>2</sup>, and R<sup>3</sup> positions (Scheme 2).

In our initial communication,<sup>6</sup> the known *t*-Bu-binerine **1a**<sup>8</sup> was found to give the highest diastereo- and enantioselectivity for the synthesis of substituted indanes (Scheme 1c). An X-ray structure of the oxidative addition complex Pd(**1a**)<sub>2</sub>PhBr revealed a short contact between the *t*-Bu group of **1a** and the ortho position of the Pd-bound substrate, thereby suggesting an important role of the P-substituent. In addition, the R<sup>1</sup> substituent at phosphorus is easy to modify, similar to R<sup>29</sup> but unlike R<sup>3</sup>, which requires a rather long synthetic sequence.<sup>10</sup> On the basis of these considerations, we directed our efforts at modifying the R<sup>1</sup> rather than the R<sup>2</sup> and R<sup>3</sup> positions.

The known binerines (*R*)-**1a–d** as well as seven new binerines (*R*)-**1e–k** were synthesized from the dilithiated precursor (*R*)-**6** (obtained from (*R*)-BINOL in three steps), either upon reaction with R<sup>1</sup>PCl<sub>2</sub> or via the chlorophosphine intermediate.<sup>11</sup> The phosphine–borane complexes **1a–k**·BH<sub>3</sub>

Scheme 2. Synthesis of Binerine Ligands in This Study<sup>a</sup>

<sup>a</sup>Route 1: R<sup>1</sup>PCl<sub>2</sub>, then BH<sub>3</sub>·THF; route 2: (i) Et<sub>2</sub>NPCl<sub>2</sub>, (ii) HCl, (iii) R<sup>1</sup>Li, then BH<sub>3</sub>·THF. <sup>b</sup>HBF<sub>4</sub>·OEt<sub>2</sub>. <sup>c</sup>*t*-BuLi, MeI, then HBF<sub>4</sub>·OEt<sub>2</sub>. <sup>d</sup>Thermal ellipsoids at the 50% probability level, most H atoms being omitted for clarity.

were initially isolated, but the DABCO-induced liberation of the free phosphine was found to be tedious, especially for the most electron-rich ligands. In addition, these free phosphines are significantly air-sensitive. To solve these issues, the corresponding phosphonium tetrafluoroborates **1a–k**·HBF<sub>4</sub> were directly prepared from the borane adducts upon treatment with HBF<sub>4</sub>·OEt<sub>2</sub> in CH<sub>2</sub>Cl<sub>2</sub>.<sup>12</sup> These binerine·HBF<sub>4</sub> salts are convenient, bench-stable precursors of free binerines that can be directly employed in the base-mediated C–H activation reaction.<sup>13</sup> This synthetic sequence can be performed on a gram-scale. As a representative example, 2 g of the original ferrocenyl-binerine **1i**·HBF<sub>4</sub> were obtained from dilithiated compound **6** in 51% overall yield.<sup>11</sup> The enantiopurity of this ligand was >99%, as determined by the HPLC analysis on a chiral phase of the corresponding borane precursor (*R*)-**1i**·BH<sub>3</sub> (the X-ray crystal structure of which is shown in Scheme 2) against its racemic mixture.<sup>11</sup> To evaluate the influence of an R<sup>2</sup> substituent on the binerine scaffold on the enantioselectivity, the new methylated ligand (*S,S,S*)-**1l**·HBF<sub>4</sub> with opposite configuration at the binaphthyl axis was prepared from the borane adduct of (*S*)-**1a** (Scheme 2).<sup>9</sup> Finally, ligand (*S*)-**1m** with a phenyl group as R<sup>3</sup> was also synthesized for comparative purposes according to the literature procedure.<sup>10</sup>

To obtain precise information on the electronic and steric properties of the synthesized ligands, the corresponding <sup>31</sup>P–<sup>77</sup>Se coupling constants were measured,<sup>15</sup> and the percent buried volumes<sup>16</sup> were calculated from the DFT-optimized oxidative addition complexes (phosphine)PdPhBr (Table 1; see also Figures S6–S10).<sup>11</sup> The electronic and steric parameters of P(*t*-Bu)<sub>3</sub>, PCy<sub>3</sub>, and PPh<sub>3</sub> are also reported for comparison

**Table 1. Electronic and Steric Parameters of Binepine Ligands**

entry	ligand	$^1J_{\text{P-Se}}$ (Hz) <sup>a</sup>	% $V_{\text{bur}}$ for Pd–P length at <sup>b</sup>	
			2.00 Å	2.28 Å
1	P( <i>t</i> -Bu) <sub>3</sub>	685	42.7	37.0
2	PCy <sub>3</sub>	673 <sup>c</sup>	37.3	32.3
3	PPh <sub>3</sub>	729 <sup>c</sup>	33.7	28.8
4	<b>1a</b>	706	35.0	30.0
5	<b>1b</b>	709	33.9	28.9
6	<b>1c</b>	728	31.5	26.6
7	<b>1d</b>	731	31.8	26.9
8	<b>1e</b>	756	31.9	27.1
9	<b>1f</b>	729	31.5	26.7
10	<b>1g</b>	705	33.3	28.3
11	<b>1h</b>	707	34.2	29.2
12	<b>1i</b>	726	34.5	29.5
13	<b>1j</b>	724	39.8	34.6
14	<b>1k</b>	707	37.3	32.3
15	<b>1l</b>	718	38.6	33.3
16	<b>1m</b>	726	34.5	29.9

<sup>a</sup> $^{31}\text{P}$ – $^{77}\text{Se}$  coupling constant measured from the  $^{31}\text{P}$  NMR spectrum of the phosphine selenides. <sup>b</sup>Percent buried volumes calculated by DFT<sup>11</sup> for (phosphine)PdPhBr complexes. <sup>c</sup>From ref 17.

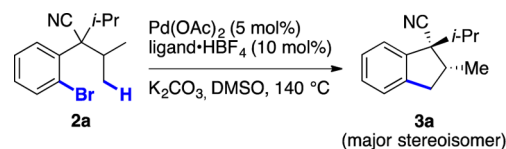
(entries 1–3). The percent  $V_{\text{bur}}$  values of P(*t*-Bu)<sub>3</sub>, PCy<sub>3</sub>, and PPh<sub>3</sub> obtained with this method are very close ( $\pm 1.5\%$ ) to those reported for the corresponding (phosphine)AuCl complexes.<sup>16</sup>

The P–Se coupling constants obtained for binepines **1a–m** indicate that all these ligands are significantly less electron-rich than P(*t*-Bu)<sub>3</sub> and PCy<sub>3</sub>.<sup>17</sup> Except for binepines with R<sup>1</sup> = *t*-Bu, Cy, *o*-Tol, 1-Naph, and *o*-Biph (entries 4, 5, 10, 11, 14), which have  $^1J_{\text{P-Se}}$  values between P(*t*-Bu)<sub>3</sub> and PPh<sub>3</sub>, and **1e**, which is significantly less basic than PPh<sub>3</sub> (entry 8), all synthesized phosphines are actually in the same range as PPh<sub>3</sub>. This is somewhat surprising because binepines have been often regarded as chiral analogues of trialkylphosphines, but the current data indicate that this perception is somewhat erroneous and that at least aryl-substituted binepines should be considered as chiral analogues of PPh<sub>3</sub>.

With respect to steric bulk, it is interesting to note that *t*-Bu, Cy, and Ph-substituted binepines **1a–c** (entries 4–6) have significantly smaller buried volumes than P(*t*-Bu)<sub>3</sub>, PCy<sub>3</sub>, and PPh<sub>3</sub> (entries 1–3), respectively. In addition to **1c**, aryl-substituted binepines **1d–i** display buried volumes that are smaller or in the same range as PPh<sub>3</sub>, (entries 7–12), including ligands **1g–i**. Even ligands **1j–k** bearing bulky 9-methylfluorenyl<sup>18</sup> or *o*-biphenyl<sup>19</sup> groups do not have much larger buried volumes (entries 13–14). Finally, ligands **1l** and **1m** containing Me or Ph groups as R<sup>2</sup> or R<sup>3</sup> are, as expected, significantly more bulky than the corresponding unsubstituted ligands **1a** and **1c** (entries 15–16). Of note, the buried volume model permits a rough steric comparison within the binepine family of ligands, but obviously it cannot be employed to predict the effects induced by R<sup>1</sup> and R<sup>3</sup> substituents on the enantioselectivity of the studied C–H activation reaction because the latter is affected by remote substrate–ligand interactions that are not taken into account in the model.

## ■ EFFECT OF BINEPINES IN ASYMMETRIC C(SP<sup>3</sup>)–H ARYLATION

The synthesized binepine-HBF<sub>4</sub> salts were evaluated on the asymmetric C–H arylation of aryl bromide **2a** under previously optimized conditions (Table 2).<sup>6</sup> Consistent with previous

**Table 2. Effect of the Structure of Binepines on the Asymmetric C(sp<sup>3</sup>)–H Arylation<sup>a</sup>**

entry	ligand	GC yield (%) <sup>b</sup>	d.r. <sup>b</sup>	e.r. <sup>c</sup>
1	( <i>R</i> )- <b>1a</b>	73	19:1	77:23
2	( <i>R</i> )- <b>1b</b>	83	21:1	77:23
3	( <i>R</i> )- <b>1c</b>	85 (82)	24:1	85:15
4	( <i>R</i> )- <b>1d</b>	63	42:1	86:14
5	( <i>R</i> )- <b>1e</b>	56	13:1	73:27
6	( <i>R</i> )- <b>1f</b>	79	19:1	86:14
7	( <i>R</i> )- <b>1g</b>	99	14:1	82:18
8	( <i>R</i> )- <b>1h</b>	28	28:1	85:15
9	( <i>R</i> )- <b>1i</b>	69 (67)	55:1	93:7
10	( <i>R</i> )- <b>1j</b>	69	12:1	85:15
11	( <i>R</i> )- <b>1k</b>	3		
12	( <i>S</i> )- <b>1l</b>	95	19:1	60:40
13	( <i>S</i> )- <b>1m</b>	75	7:1	19:81

<sup>a</sup>The absolute configuration of the shown major stereoisomer of **3a** was ascribed as described in Scheme 3. <sup>b</sup>Determined by GC/MS using tetradecane as the internal standard. Yield of the isolated product in parentheses. <sup>c</sup>Determined by HPLC using a chiral phase.

results, *t*-Bu and Cy binepines **1a–b** furnished indane **3a** in good diastereoselectivity and 77:23 e.r. (entries 1–2). Under the same conditions, we were surprised to find that Ph-substituted binepine **1c** gave a higher d.r. and e.r. (entry 3). Other P-substituted binepines gave variable results (entries 4–11). The most interesting stereoselectivities were obtained with ferrocenylbinepine **1i** (entry 9), which furnished **3a** in good yield, high diastereoselectivity (d.r. 55:1) and enantioselectivity (93:7). Of note, ligand **1l** with the opposite (*S*) axial configuration and R<sup>2</sup> = Me provided the same major enantiomer of **3a**, but with a low e.r. (entry 12). Finally, ligand (*S*)-**1m** with R<sup>3</sup> = Ph induced the same sense of enantioselectivity, but the e.r. was not improved compared with the parent ligand **1c** with R<sup>3</sup> = H (entry 13). These results somewhat validate our initial choice to focus our efforts on the modification of the phosphorus substituent.

In parallel, we reexamined the effect of the basic system in this reaction. Indeed, our initial optimized conditions involved Pd(OAc)<sub>2</sub> as the palladium source and K<sub>2</sub>CO<sub>3</sub> as the base (Table 2). However, in a polar solvent such as DMSO, both acetate and carbonate are able to act as the active base in the C–H activation step that proceeds through the concerted metalation–deprotonation mechanism.<sup>20,21</sup> To lift this ambiguity, different bases were tested in combination with Pd<sub>2</sub>dba<sub>3</sub> as the Pd source and **1c** as the chiral ligand (Table 3). In the presence of KOAc as the sole base, a marked decrease of both the d.r. and the e.r. was observed (entry 2) compared with the Pd(OAc)<sub>2</sub>/K<sub>2</sub>CO<sub>3</sub> combination (entry 1). In contrast, with K<sub>2</sub>CO<sub>3</sub> alone, slightly higher d.r. and e.r. were observed compared with the Pd(OAc)<sub>2</sub>/K<sub>2</sub>CO<sub>3</sub> mixture (entry 3). These

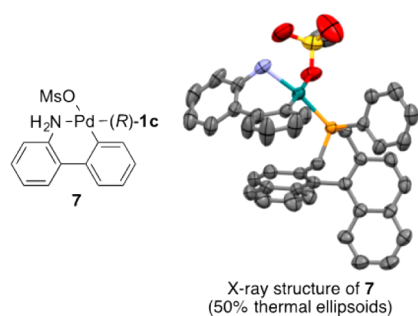
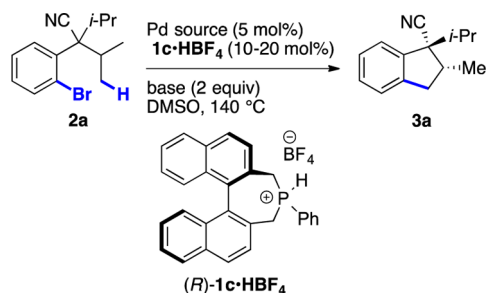


**Table 3. Effect of the Base on the Asymmetric C(sp<sup>3</sup>)-H Arylation**



entry	Pd source <sup>a</sup>	base	d.r. <sup>b</sup>	e.r. <sup>c</sup>
1	Pd(OAc) <sub>2</sub>	K <sub>2</sub> CO <sub>3</sub>	24:1	85:15
2	Pd <sub>2</sub> dba <sub>3</sub>	KOAc	9:1	75:25
3	Pd <sub>2</sub> dba <sub>3</sub>	K <sub>2</sub> CO <sub>3</sub>	34:1	87:13
4	Pd <sub>2</sub> dba <sub>3</sub>	Na <sub>2</sub> CO <sub>3</sub>	23:1	80:20
5	Pd <sub>2</sub> dba <sub>3</sub>	Rb <sub>2</sub> CO <sub>3</sub>	42:1	87:13
6	Pd <sub>2</sub> dba <sub>3</sub>	Cs <sub>2</sub> CO <sub>3</sub>	51:1	89:11
7	Pd <sub>2</sub> dba <sub>3</sub>	K <sub>3</sub> PO <sub>4</sub>	36:1	84:16
8	Pd <sub>2</sub> dba <sub>3</sub>	KOPiv	6:1	72:28
9 <sup>d</sup>	Pd <sub>2</sub> dba <sub>3</sub>	KOPiv	4:1	58:42
10 <sup>e</sup>	<b>7</b>	K <sub>2</sub> CO <sub>3</sub>	47:1	90:10

<sup>a</sup>20 mol % ligand were used with Pd(OAc)<sub>2</sub> and 10 mol % with Pd<sub>2</sub>dba<sub>3</sub>. <sup>b</sup>Determined by GC/MS using tetradecane as the internal standard. <sup>c</sup>Determined by HPLC using a chiral phase. <sup>d</sup>With mesitylene instead of DMSO as the solvent. <sup>e</sup>With precatalyst **7** instead of Pd<sub>2</sub>dba<sub>3</sub>/(*R*)-**1c**·HBF<sub>4</sub> and 100 °C instead of 140 °C.

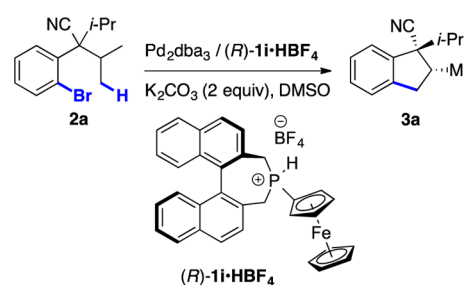
observations show not only that carbonate is the active base in this reaction performed in a polar solvent such as DMSO, but also that carbonate furnishes higher stereoselectivities than acetate. Thus, the catalytic amount of acetate introduced when Pd(OAc)<sub>2</sub> is employed as the Pd source can be only detrimental to the stereoselectivity. Another clear advantage of using Pd<sub>2</sub>dba<sub>3</sub> instead of Pd(OAc)<sub>2</sub> is the fact that the latter requires sacrificing 1 equiv of precious chiral ligand to generate the active Pd<sup>0</sup> catalyst.

Other carbonate bases were then tested in combination with Pd<sub>2</sub>dba<sub>3</sub> (entries 4–6). The highest stereoselectivities were obtained with Cs<sub>2</sub>CO<sub>3</sub> (entry 6). However, the difference between Cs<sub>2</sub>CO<sub>3</sub> and K<sub>2</sub>CO<sub>3</sub> was less pronounced under the final optimized conditions (vide infra), and thus, the cheaper K<sub>2</sub>CO<sub>3</sub> was chosen for scope studies. Interestingly, potassium phosphate was also found to be a competent base for this reaction (entry 7). Pivalate, which is widely employed as the active base in C(sp<sup>3</sup>)-H activation reactions,<sup>2–4</sup> behaved similarly to acetate and was less selective than carbonate (entry 8). This effect was even more pronounced when mesitylene was used instead of DMSO as the solvent (entry 9), thereby showing the dramatic impact of the base/solvent combination

on the stereoselectivity in the current reaction. Finally, the well-defined Buchwald-Tudge-type<sup>22</sup> precatalyst **7**, which was readily synthesized from (*R*)-**1c**·HBF<sub>4</sub> and which should generate the corresponding monoligated Pd<sup>0</sup>-L complex under the current basic reaction conditions, gave results similar to the Pd<sub>2</sub>dba<sub>3</sub>/**1c** in situ combination (entry 10).

This major effect of the base being clarified, the reaction conditions were refined (Table 4). Gratifyingly, the combina-

**Table 4. Final Optimization of the Asymmetric C(sp<sup>3</sup>)-H Arylation**



entry	mol % Pd <sub>2</sub> (dba) <sub>3</sub>	mol % <b>li</b>	temp (°C)	yield (%) <sup>a</sup>	d.r. <sup>b</sup>	e.r. <sup>c</sup>
1	2.5	10	140	75	65:1	94:6
2	2.5	7.5	90	87	≥99:1	96:4
3	2.5	7.5	80	48	≥99:1	95:5
4	1	3	90	96	89:1	96:4
5	0.5	1.5	90	88	80:1	95:5
6	<i>d</i>	<i>d</i>	90	10 (67) <sup>e</sup>	18:1	

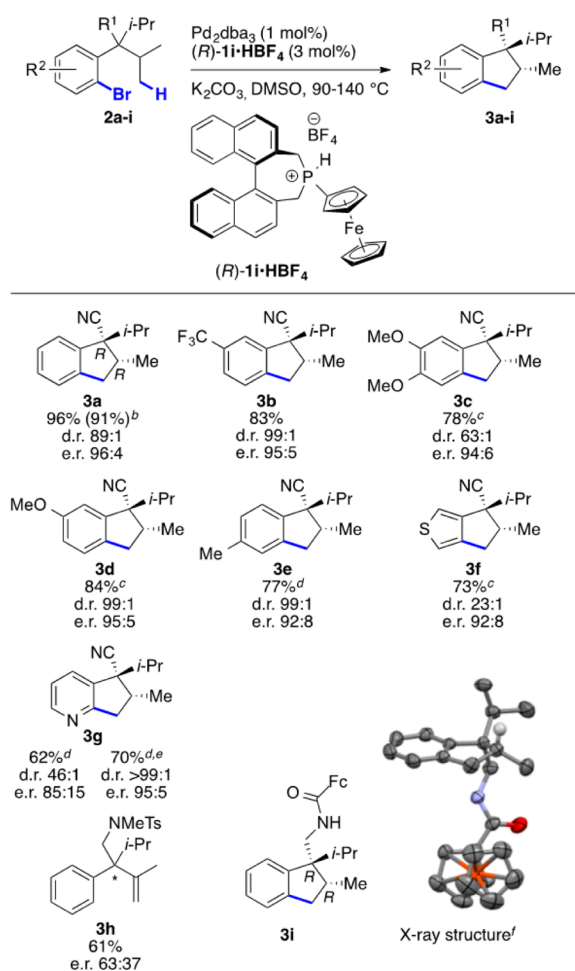
<sup>a</sup>Yield of the isolated product. <sup>b</sup>Determined by GC/MS using tetradecane as the internal standard. <sup>c</sup>Determined by HPLC using a chiral phase. <sup>d</sup>Reaction performed with Pd(PPh<sub>3</sub>)<sub>4</sub> (5 mol %) as the catalyst. <sup>e</sup>Reaction performed at 140 °C.

tion of binepine **1i** with Pd<sub>2</sub>dba<sub>3</sub> and K<sub>2</sub>CO<sub>3</sub> under acetate-free conditions allowed achievement of high diastereo- and enantioselectivity (entry 1). Remarkably, the temperature could be reduced to 90 °C with a slight increase in stereoselectivity (entry 2), but the reactivity dropped below this temperature (entry 3). Moreover, we were able to reduce the catalyst loading to 1 mol % Pd and 1.5 mol % ligand (entries 4–5), while retaining similar levels of stereoselectivity. This level of efficiency and stereoselectivity at such a mild temperature is unprecedented in this type of reactions.<sup>4–6</sup> In addition, a control experiment with Pd(PPh<sub>3</sub>)<sub>4</sub> as catalyst showed the superior activity of the binepine-based catalyst that promotes the reaction at 90 °C, whereas the former is active only at higher temperatures (entry 6).

## SCOPE EXTENSION

The scope of the methyl activation/intramolecular arylation was next examined employing 1 mol % Pd<sub>2</sub>dba<sub>3</sub> and 3 mol % ligand (Scheme 3). Good yields, diastereo-, and enantioselectivities were achieved for indanes **3a–e** bearing various types of substituents on the benzene ring and for fused thiophene-cyclopentane **3f**, with an e.r. in the range 92:8–96:4 and excellent diastereoselectivities. Importantly, the reaction of **2a** was performed with equal efficiency and selectivity on gram scale, thereby demonstrating the robustness of this method. For compounds **3c**, **3d**, and **3f**, the reaction had to be conducted at 140 °C to reach full conversion. The reaction of bromopyridine **2g** was found to be less selective with **1i** as the ligand, but gratifyingly, the use of 9-methylfluorenyl analogue **1j** (see



Scheme 3. Scope of the Asymmetric Arylation of Primary C–H Bonds<sup>a</sup>

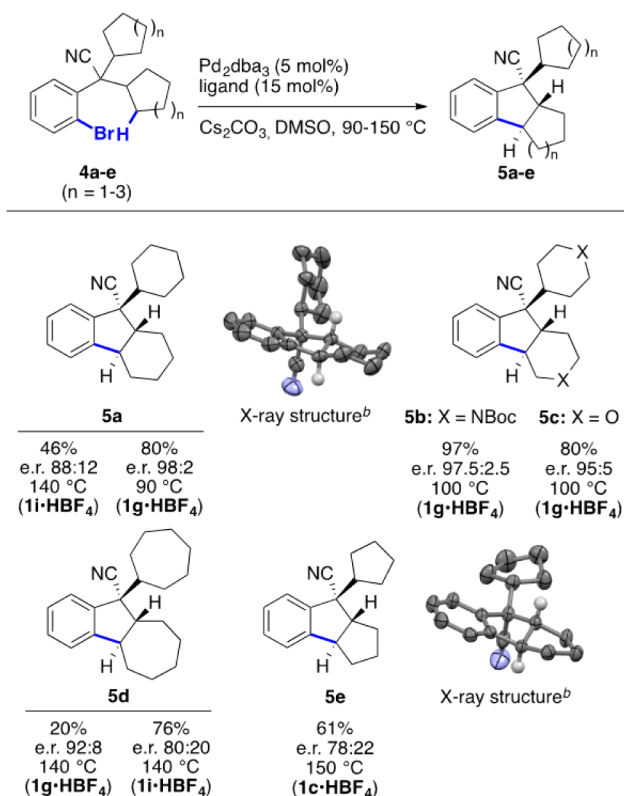
<sup>a</sup>Yields refer to the isolated product; d.r. determined by GC/MS using tetradecane as the internal standard; e.r. determined by HPLC using a chiral phase. The corresponding racemic products were obtained using  $\text{P}(\text{Cyp})_3$  as the ligand.<sup>11</sup> The absolute configurations of the shown major stereoisomers were deduced from that of **3a**. <sup>b</sup>Reaction performed on 1.9 g of substrate **2a**. <sup>c</sup>Reaction performed at  $140\text{ }^\circ\text{C}$ . <sup>d</sup>Reaction performed at  $120\text{ }^\circ\text{C}$ . <sup>e</sup>Reaction performed with **1j-HBF<sub>4</sub>** instead of **1i-HBF<sub>4</sub>**. <sup>f</sup>Thermal ellipsoids at the 50% probability level, most H atoms being omitted for clarity.

Scheme 2) allowed restoration of high levels of stereoselectivity for the formation of **3g** at  $120\text{ }^\circ\text{C}$ . Interestingly, the reaction turned out to be very sensitive to the nature of the  $\text{R}^1$  substituent at the benzylic position. For instance, the reaction of compound **2h** bearing a  $\text{CH}_2\text{N}(\text{Ts})\text{Me}$  group instead of CN gave rise to olefin **3h**,<sup>2a,b</sup> not to the corresponding indane product. This olefin was obtained in low but significant (e.r. 63:37) enantioselectivity. This promising result opens the way for the enantioselective synthesis of olefins adjacent to a quaternary carbon after further optimization.

Of note, the  $R,R$  absolute configuration of **3a** was deduced from the X-ray diffraction analysis of its derivative **3i**, obtained through reduction of the nitrile group and amide formation with ferrocenecarboxylic acid. The latter introduces a ferrocene moiety in the structure that both improves the crystallization properties and allows determination of the absolute configuration with high precision (Flack parameter  $\alpha = 0.006(12)$ ), and we believe that this system represents a useful alternative to

other derivatization methods for the determination of absolute configuration.<sup>23</sup> The same configuration was ascribed to analogues **3b–g** based on this assignment.<sup>24</sup>

Next, we turned our attention to the activation of secondary C–H bonds by examining the reaction of substrates **4a–e** bearing enantiotopic cycloalkanes (Scheme 4). This is a

Scheme 4. Asymmetric Arylation of Secondary C–H Bonds<sup>a</sup>

<sup>a</sup>Yields refer to the isolated product; d.r. determined by GC/MS using tetradecane as the internal standard; e.r. determined by HPLC using a chiral phase. The corresponding racemic products were obtained using  $\text{Pd}(\text{PPh}_3)_4$  as catalyst.<sup>11</sup> The absolute configuration of the shown major enantiomers was ascribed by analogy with that of **3a**, and their relative configuration was deduced from the shown X-ray structures. <sup>b</sup>Relative structure of the enantioenriched (**5a**) or racemic (**5e**) compound, with thermal ellipsoids at the 50% probability level, most H atoms being omitted for clarity.

somewhat more challenging case because secondary C–H bonds are supposed to be less reactive than primary ones with regard to the base-mediated C–H activation mechanism.<sup>2d</sup> Indeed, only a few cases of noncyclopropane, nonbenzylic methylene C–H activation under palladium(0) catalysis have been reported in the literature.<sup>2a,b,3d,4a,c,d,f,25</sup> In contrast to methyl activation, ferrocenyl ligand **1i** furnished disappointing results in the reaction of dicyclohexyl substrate **4a** (46% yield, e.r. 88:12). Fortunately, we found that *o*-tolyl-substituted ligand **1g** (see Scheme 2) restored both reactivity (80% yield) and high enantioselectivity (e.r. 98:2) at  $90\text{ }^\circ\text{C}$ . Remarkably, although the corresponding fused tricyclic product **5a** now contains three contiguous stereocenters, only one diastereoisomer was observed in this case, as well as for related products **5b–e**. The relative configuration of **5a** was ascribed by X-ray crystallographic analysis (Scheme 4), and the shown absolute configuration was ascribed in analogy to that of **3a**.

Compounds **4b–c** bearing heterocyclic six-membered rings provided similarly satisfying results with binepine **1g** as the ligand.

The reactions of the higher (**4d**) and lower (**4e**) homologues of **4a** were found to be more challenging. Indeed, the reaction of **4d** was sluggish with binepine **1g** (incomplete conversion, 20% yield), even at a higher temperature (140 °C). The use of ferrocenylbinepine **1i** restored reactivity (76% yield), but the enantioselectivity was lower (e.r. = 80:20) than with **1g** (e.r. = 92:8). In the case of dicyclopentyl substrate **4e**, all bulky ligands, such as **1g** and **1i** failed to give useful conversions, and only the smaller Ph-substituted binepine **1c** gave significant, albeit moderate, results (e.r. = 78:22). These and previous observations point to the high sensitivity of this reaction to substrate modifications close to the activated C–H bond. Fortunately, the high modularity of binepine ligands allowed us to achieve high stereoselectivity in most cases by simply testing a small number of analogues. The relative configuration of **5e** was found to be identical to that of **5a** by X-ray diffraction analysis (Scheme 4). Interestingly, **5e** displays the unusual, contrathermodynamic trans-5,5 ring junction.<sup>26</sup>

## MECHANISTIC CONSIDERATIONS

All previous theoretical studies on Pd<sup>0</sup>-catalyzed C(sp<sup>3</sup>)–H activation reactions were performed considering a monoligated (PdL) species in the C–H activation step;<sup>2c,d,i,3c,e,4f,g,20,27</sup> however, we were puzzled by the reported reactivity and enantioselectivity of the bidentate phosphines Me-Duphos<sup>4b</sup> and Josiphos<sup>6</sup> in similar transformations, raising the possibility of an alternative C–H activation mode from a bis-ligated (PdL<sub>2</sub>) species, in line with a previous study on Pd<sup>0</sup>-catalyzed C(sp<sup>2</sup>)–H activation.<sup>28,29</sup> In addition, binepines are not particularly bulky, as shown above with their calculated buried volumes, and they commonly adopt ML<sub>2</sub> coordination modes in other catalytic reactions.<sup>7</sup> To get more insight on the nature of the active species formed with binepines in the current reaction, we studied the linearity of the ee of indane **3a** vs the ee of ferrocenylbinepine **1i** (Figure 1). A linear correlation was found, which is indicative of the monoligated nature of the Pd complex involved in the enantiodetermining C–H activation step.<sup>30,31</sup> This would also be consistent with the experiment performed with precatalyst **7**, which showed results similar to

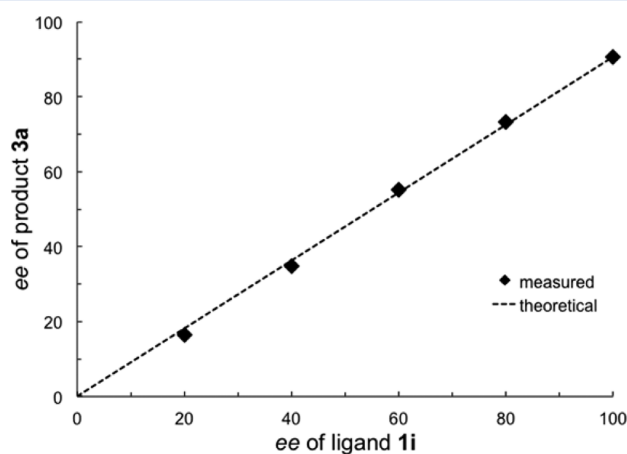
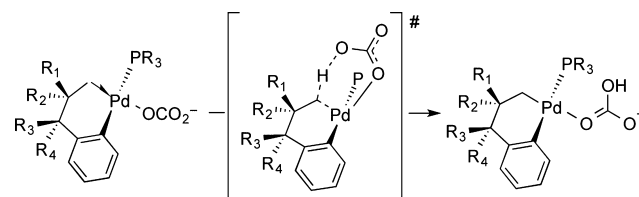


**Figure 1.** Linearity of the enantiomeric excess of product **3a** vs that of ligand **1i**. Experiments were conducted under conditions described in Scheme 3.<sup>11</sup>

the corresponding in situ Pd/ligand mixture (Table 3, entry 10).

On the basis of these elements, it seems reasonable to propose that the enantiodetermining C–H activation step involves a monoligated Pd species in the present case, as well. Only a handful of studies have dealt with catalytic enantioselective C(sp<sup>3</sup>)–H activation processes from a computational perspective.<sup>4f,g</sup> In previous studies, we have shown that the geometry imposed by the C–Br oxidative addition of the substrate to the palladium center induces a preferential geometry for the coordination of the base.<sup>2c,d,20</sup> The newly formed Pd–C(sp<sup>2</sup>) bond is trans to the phosphine ligand and the base is coordinated trans to a C(sp<sup>3</sup>)–H agostic interaction (Scheme 5). In the transition state of the C–H

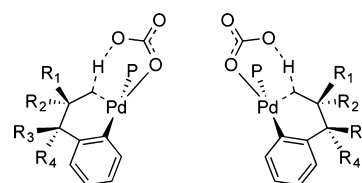
## Scheme 5. Computed Base-Assisted C–H Activation



activation, the O–Pd–C(sp<sup>3</sup>) angle is reduced to ~120° for a noncoordinated oxygen atom to abstract the hydrogen atom in an AMLA(6) process,<sup>32</sup> thereby putting the carbonate ligand above the initial coordination plane.

For an achiral phosphine such as PPh<sub>3</sub>, the two enantiomeric transition states in Scheme 6 have the same energy, and racemic

## Scheme 6. Enantiomeric Transition States for C–H Activation



mixtures are obtained for any distribution of the R<sup>1</sup>–R<sup>4</sup> substituents. However, the energy of the six-membered palladacycle that is formed in the transition state is strongly influenced by the actual nature of the R<sup>1</sup>–R<sup>4</sup> substituents. This leads to the selective formation of one diastereoisomer, as shown previously (Table 4, entry 6).<sup>2b,d</sup> The indane diastereoisomer with the Me group cis to the CN group is favored over the diastereoisomer with Me cis to *i*-Pr by a ratio of 18:1, roughly identical to the d.r. observed when binepine (*R*)-**1a** is used as the phosphine ligand (Table 2, entry 1).

With a chiral phosphine, the two transition states in Scheme 6 are diastereoisomeric, and therefore, they do not have the same energy. This induces selective formation of one enantiomer; however, the energy penalty imposed on one enantiomer by the chiral phosphine is expected to be lower than the penalty imposed by the relative position of the various substituents on the six-membered palladacycle. With four different substituents, R<sup>1</sup>–R<sup>4</sup>, a total of eight different transition states should be considered for the C–H activation catalyzed by Pd[(*R*)-**1a**]. Indeed, the respective positions of the four substituents generate four different palladacycles, and the carbonate base can promote the C–H activation either from

the top of the forming palladacycle (as shown in Scheme 6) or from the bottom.

Geometry optimizations have been carried out in the gas phase for the eight possible transition states in the case of binepine (*R*)-**1a**,<sup>33</sup> using the hybrid PBE0 functional<sup>34</sup> and the D3(bj) correction as implemented by Grimme.<sup>35</sup> The influence of the solvent (DMSO) was taken into consideration through single-point calculations on the gas-phase optimized geometry within the SMD model.<sup>36</sup> The various transition state structures are labeled according to the configuration of the corresponding indane product (first *R* or *S* label for the carbon substituted by CN) and according to the geometry of the attack by the base (up or down, the representation in Scheme 5 defining up). Table 5 collects the relative Gibbs free energies of the various

**Table 5. Relative Gibbs Free Energies (kcal mol<sup>-1</sup>, 413 K) of the Various Transition States for C–H Activation**

	$\Delta\Delta G^\ddagger$		$\Delta\Delta G^\ddagger$
<i>R</i> - <i>R</i> -up	0.0	<i>R</i> - <i>R</i> -down	16.0
<i>S</i> - <i>S</i> -down	1.0	<i>S</i> - <i>S</i> -up	14.3
<i>R</i> - <i>S</i> -up	3.8	<i>R</i> - <i>S</i> -down	9.1
<i>S</i> - <i>R</i> -down	7.5	<i>S</i> - <i>R</i> -up	11.0

transition states computed in DMSO at 413 K (the geometries of the various TS are available in a single .xyz file in the Supporting Information).<sup>11</sup>

From Table 5, there appear to be two groups of values for the relative energies of the transition states. The highest values are all associated with transition state structures in which the cyano group is in an axial position in the forming six-membered palladacycle, facing the carbonate base. In these structures, the isopropyl group experiences a gauche interaction with the vicinal methyl group, as well as allylic strain with the aromatic ring, thus leading to significant steric repulsion.

For the four other cases, in which the isopropyl group occupies the axial position facing the carbonate, the stereoisomers with Me cis to CN, that is, *R*-*R*-up and *S*-*S*-down, are computed to be significantly favored over the stereoisomers with Me trans to CN, that is, *R*-*S*-up and *S*-*R*-down, as observed experimentally. The  $\Delta\Delta G^\ddagger$  value of 3.8 kcal mol<sup>-1</sup> translates to a kinetic preference for the formation of *R*-*R*-up with respect to *R*-*S*-up of ~100:1, in qualitative agreement with the experimental observations. The calculations do reproduce the kinetic preference to form a specific couple of enantiomers. In addition, the  $\Delta\Delta G^\ddagger$  value of 1.0 kcal mol<sup>-1</sup> computed between the transition states *R*-*R*-up and *S*-*S*-down translates into an e.r. of 77:23 at 413 K, in excellent agreement with experiment (Table 2).<sup>37</sup> Of note, the activation barrier between the lowest transition state, *R*-*R*-up, and the corresponding agostic complex was computed to be  $\Delta G^\ddagger = 15.7$  kcal mol<sup>-1</sup> (at 413 K), which is a significantly lower value than those computed for similar reactions (typically around 25 kcal mol<sup>-1</sup>).<sup>2d,3e,4f</sup> This is in qualitative agreement with the fact that the current ligand/base/solvent system allows one to perform the reaction at a lower temperature (363 K).

The main difference between the two transition state geometries, *R*-*R*-up and *S*-*S*-down, is the orientation of the phosphine ligand with respect to the base + substrate ensemble (Figure 2). In *R*-*R*-up, the *t*-Bu group on the phosphine is facing the carbonate, and two C–H···O short contacts are present (2.189 and 2.341 Å). There is also a short C–H···O contact of 2.328 Å between the axial isopropyl group and the

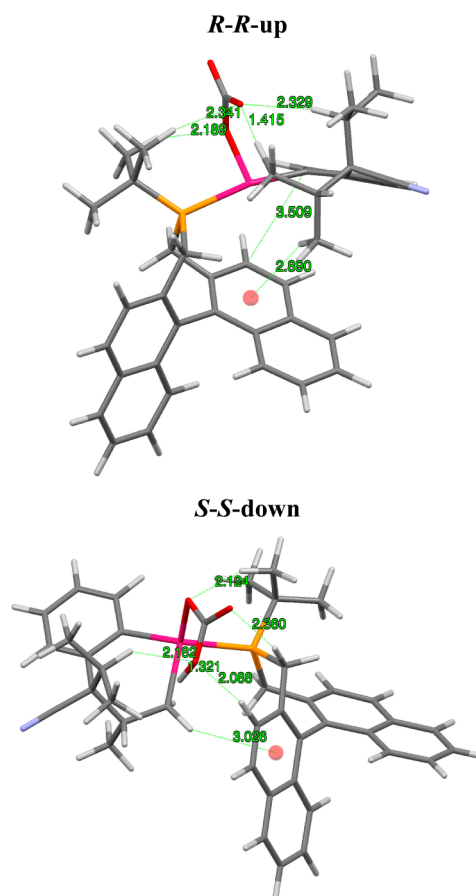


**Figure 2.** Optimized geometry of the two lowest transition state structures, *R*-*R*-up and *S*-*S*-down, showing selected short contacts.

carbonate. These short contacts are to be compared with the O···H bond distance of 1.415 Å between the oxygen atom and the abstracted hydrogen atom. In this orientation of the phosphine, one naphthyl group is located below the substrate, and the shortest C···C contact between this naphthyl group and the aromatic ring of the substrate is 3.509 Å. In addition, the nonactivated methyl group of the isopropyl group undergoing C–H activation presents a C–H··· $\pi$  interaction with the naphthyl group, as illustrated by the distance of 2.890 Å between the proximal hydrogen atom and the centroid of one aromatic ring of the naphthyl (Figure 2). All these contacts are associated with weakly stabilizing nonbonding interactions, as illustrated by the noncovalent interaction (NCI) maps between the phosphine ligand and the base + substrate ensemble shown in Figure 3.<sup>11</sup>

In *S*-*S*-down, the situation is significantly different. The binepine ligand does not display the same kind of stabilizing network of short contacts as observed in *R*-*R*-up (Figure 2). The short contacts between the carbonate and the hydrogen atoms on the phosphine ligand are distributed on the *t*-Bu group (2.124 Å), a bridging methylene (2.360 Å), and a naphthyl group (2.088 Å). In addition, the isopropyl group of the substrate also shows a short C–H···O contact of 2.182 Å. In *S*-*S*-down, the forming O···H bond (1.321 Å) is much more advanced than in *R*-*R*-up. This network of contacts sets the global positioning of the phosphine ligand and prevents the establishment of any significant C–H··· $\pi$  or stacking interaction between the substrate and the naphthyl groups of the ligand, as illustrated by the longer contact (3.06 Å) between a C–H bond



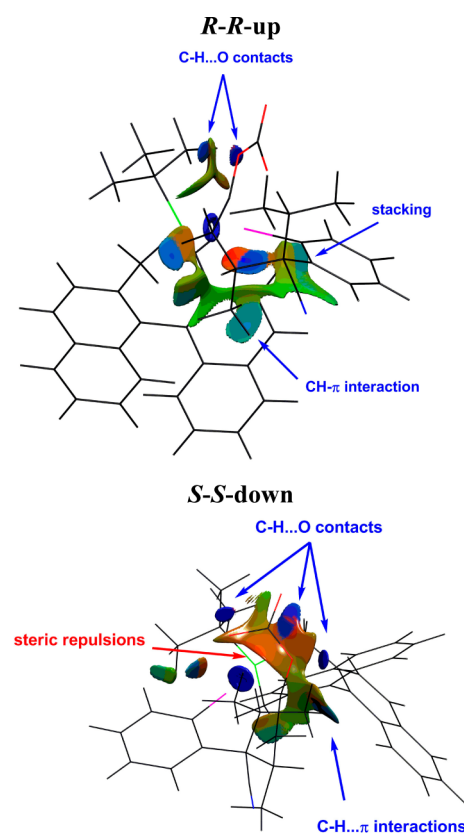


**Figure 3.** NCI maps of weak interactions between the phosphine ligand and the base + substrate ensemble.<sup>11</sup> Only intermolecular maps using promolecular densities are shown, and the blue regions are associated with slightly attractive weak interactions, whereas the red regions are associated with repulsive interactions.

of the activated methyl group and the centroid of the proximal aromatic ring of the ligand. Contrary to what is observed on the NCI maps for **R-R-up**, in the case of **S-S-down**, a significant region of slightly repulsive interactions is developing between the phosphine ligand and the base + substrate ensemble. Even though these NCI plots present only qualitative behavior, they clearly show that significantly different networks of interactions between the reactive center and the phosphine ligand are operating in the two transition states. It is interesting to note that the favored transition state features mostly stabilizing interactions, albeit weak in magnitude.

## CONCLUSION

We have synthesized new binepine ligands that provide high diastereo- and enantioselectivity in the intramolecular arylation of primary and secondary C(sp<sup>3</sup>)-H bonds, giving rise to fused cyclopentanes. The ligands were obtained as bench-stable phosphonium tetrafluoroborate salts that can be directly employed in catalysis under basic conditions. It was shown that a ferrocenyl P-substituent on the ligand allows achievement of high stereoselectivities in combination with potassium carbonate in DMSO for the arylation of primary C-H bonds, under unprecedentedly low temperature (90 °C) and catalyst loading (1–2 mol % Pd/2–3 mol % ligand). Using Pd<sub>2</sub>dba<sub>3</sub> as a base-free precatalyst, carbonate was shown to be the active base and to provide higher stereoselectivities than acetate and pivalate. The more difficult arylation of secondary C-H bonds could also be achieved and required fine-tuning of

the ligand structure and the carbonate counteranion. This allowed us to generate polycyclic products containing three adjacent stereocenters as single diastereoisomers and with moderate to high enantioselectivity. Experimental data indicated that the enantiodetermining C-H activation step involves a monoligated species. DFT (PBE0-D3) calculations performed with binepine (**R**)-**1a** reproduced well the experimental enantiomeric ratio. The preferred formation of the (**R,R**) indane enantiomer was attributed to the establishment of a more efficient network of stabilizing weak interactions between the phosphine and the base + substrate ensemble in the transition state.

## ASSOCIATED CONTENT

### Supporting Information

The Supporting Information is available free of charge on the ACS Publications website at DOI: 10.1021/acscatal.5b00898.

Full characterization of all new compounds, detailed experimental procedures, Cartesian coordinates, electronic and Gibbs free energies for the systems computed (PDF)

NMR spectra and HPLC analyses for target molecules (PDF)

Rotatable structure images of the various TS (XYZ)

X-ray crystallographic (CIF) data (CIF)

## AUTHOR INFORMATION

### Corresponding Authors

\*E-mail: clot@univ-montp2.fr.

\*E-mail: olivier.baudoin@univ-lyon1.fr.

### Notes

The authors declare no competing financial interest.

## ACKNOWLEDGMENTS

We thank the Ministère de l'Enseignement Supérieur et de la Recherche and Institut Universitaire de France for financial support, and CCIR-ICBMS (Université Claude Bernard Lyon 1) for the allocation of computational resources.

## REFERENCES

- (a) Jazzar, R.; Hitce, J.; Renaudat, A.; Sofack-Kreutzer, J.; Baudoin, O. *Chem. - Eur. J.* **2010**, *16*, 2654–2672. (b) Baudoin, O. *Chem. Soc. Rev.* **2011**, *40*, 4902–4911. (c) Li, H.; Li, B.-J.; Shi, Z.-J. *Catal. Sci. Technol.* **2011**, *1*, 191–206. (d) Dastbaravardeh, N.; Christakakou, M.; Haider, M.; Schnürch, M. *Synthesis* **2014**, *46*, 1421–1439.
- (a) Baudoin, O.; Herrbach, A.; Guéritte, F. *Angew. Chem., Int. Ed.* **2003**, *42*, 5736–5740. (b) Hitce, J.; Retailleau, P.; Baudoin, O. *Chem. - Eur. J.* **2007**, *13*, 792–799. (c) Chaumontet, M.; Piccardi, R.; Audic, N.; Hitce, J.; Peglion, J.-L.; Clot, E.; Baudoin, O. *J. Am. Chem. Soc.* **2008**, *130*, 15157–15166. (d) Rousseaux, S.; Davi, M.; Sofack-Kreutzer, J.; Pierre, C.; Kefalidis, C. E.; Clot, E.; Fagnou, K.; Baudoin, O. *J. Am. Chem. Soc.* **2010**, *132*, 10706–10716. (e) Pierre, C.; Baudoin, O. *Org. Lett.* **2011**, *13*, 1816–1819. (f) Guyonnet, M.; Baudoin, O. *Org. Lett.* **2012**, *14*, 398–401. (g) Sofack-Kreutzer, J.; Martin, N.; Renaudat, A.; Jazzar, R.; Baudoin, O. *Angew. Chem., Int. Ed.* **2012**, *51*, 10399–10402. (h) Janody, S.; Jazzar, R.; Comte, A.; Holstein, P. M.; Vors, J.-P.; Ford, M. J.; Baudoin, O. *Chem. - Eur. J.* **2014**, *20*, 11084–11090. (i) Kefalidis, C. E.; Davi, M.; Holstein, P. M.; Clot, E.; Baudoin, O. *J. Org. Chem.* **2014**, *79*, 11903–11911. (j) Dailler, D.; Danoun, G.; Baudoin, O. *Angew. Chem., Int. Ed.* **2015**, *54*, 4919–4922.
- (3) Selected examples: (a) Dong, C.-G.; Hu, Q.-S. *Angew. Chem., Int. Ed.* **2006**, *45*, 2289–2292. (b) Ren, H.; Knochel, P. *Angew. Chem., Int. Ed.* **2006**, *45*, 3462–3465. (c) Lafrance, M.; Gorelsky, S. I.; Fagnou, K.



- J. Am. Chem. Soc.* **2007**, *129*, 14570–14571. (d) Watanabe, T.; Oishi, S.; Fujii, N.; Ohno, H. *Org. Lett.* **2008**, *10*, 1759–1762. (e) Rousseaux, S.; Gorelsky, S. I.; Chung, B. K. W.; Fagnou, K. *J. Am. Chem. Soc.* **2010**, *132*, 10692–10705. (f) Tsukano, C.; Okuno, M.; Takemoto, Y. *Angew. Chem., Int. Ed.* **2012**, *51*, 2763–2766. (g) Piou, T.; Neuville, L.; Zhu, J. *Angew. Chem., Int. Ed.* **2012**, *51*, 11561–11565. (h) Yan, J.-X.; Li, H.; Liu, X.-W.; Shi, J.-L.; Wang, X.; Shi, Z.-J. *Angew. Chem., Int. Ed.* **2014**, *53*, 4945–4949. For pioneering work: (i) Dyker, G. *Angew. Chem., Int. Ed. Engl.* **1992**, *31*, 1023–1025. (j) Dyker, G. *Angew. Chem., Int. Ed. Engl.* **1994**, *33*, 103–105. (k) Catellani, M.; Motti, E.; Ghelli, S. *Chem. Commun.* **2000**, *46*, 2003–2004.
- (4) (a) Nakanishi, M.; Katayev, D.; Besnard, C.; Kündig, E. P. *Angew. Chem., Int. Ed.* **2011**, *50*, 7438–7441. (b) Anas, S.; Cordi, A.; Kagan, H. B. *Chem. Commun.* **2011**, *47*, 11483–11485. (c) Saget, T.; Lemouzy, S. J.; Cramer, N. *Angew. Chem., Int. Ed.* **2012**, *51*, 2238–2242. (d) Katayev, D.; Nakanishi, M.; Bürgi, T.; Kündig, E. P. *Chem. Sci.* **2012**, *3*, 1422–1425. (e) Donets, P. A.; Saget, T.; Cramer, N. *Organometallics* **2012**, *31*, 8040–8046. (f) Larionov, E.; Nakanishi, M.; Katayev, D.; Besnard, C.; Kündig, E. P. *Chem. Sci.* **2013**, *4*, 1995–2005. (g) Katayev, D.; Larionov, E.; Nakanishi, M.; Besnard, C.; Kündig, E. P. *Chem. - Eur. J.* **2014**, *20*, 15021–15030.
- (5) (a) Saget, T.; Cramer, N. *Angew. Chem., Int. Ed.* **2012**, *51*, 12842–12845. For a more recent study on the enantioselective synthesis of b-lactams also using phosphoramidites: (b) Pedroni, J.; Boghi, M.; Saget, T.; Cramer, N. *Angew. Chem., Int. Ed.* **2014**, *53*, 9064–9067.
- (6) Martin, N.; Pierre, C.; Davi, M.; Jazzar, R.; Baudoin, O. *Chem. - Eur. J.* **2012**, *18*, 4480–4484.
- (7) Gladiali, S.; Alberico, E.; Junge, K.; Beller, M. *Chem. Soc. Rev.* **2011**, *40*, 3744–3763.
- (8) (a) Chi, Y.; Zhang, X. *Tetrahedron Lett.* **2002**, *43*, 4849–4852. (b) Junge, K.; Oehme, G.; Monsees, A.; Riermeier, T.; Dingerdissen, U.; Beller, M. *Tetrahedron Lett.* **2002**, *43*, 4977–4980. (c) Junge, K.; Hagemann, B.; Enthaler, S.; Spannenberg, A.; Michalik, M.; Oehme, G.; Monsees, A.; Riermeier, T.; Beller, M. *Tetrahedron: Asymmetry* **2004**, *15*, 2621–2631.
- (9) (a) Kasák, P.; Arion, V. B.; Widhalm, M. *Tetrahedron: Asymmetry* **2006**, *17*, 3084–3090. (b) Nareddy, P.; Mantilli, L.; Guénee, L.; Mazet, C. *Angew. Chem., Int. Ed.* **2012**, *51*, 3826–3831.
- (10) Fujiwara, Y.; Fu, G. C. *J. Am. Chem. Soc.* **2011**, *133*, 12293–12297.
- (11) See the [Supporting Information](#) for details.
- (12) (a) McKinsty, L.; Livinghouse, T. *Tetrahedron* **1995**, *51*, 7655–7666. (b) Denmark, S. E.; Werner, N. S. *Org. Lett.* **2011**, *13*, 4596–4599.
- (13) Wurz, R. P.; Fu, G. C. *J. Am. Chem. Soc.* **2005**, *127*, 12234–12235.
- (14) For a related bis(binopine)ferrocene ligand: Xiao, D.; Zhang, X. *Angew. Chem., Int. Ed.* **2001**, *40*, 3425–3428.
- (15) Allen, D. W.; Taylor, B. F. *J. Chem. Soc., Dalton Trans.* **1982**, 51–54.
- (16) Clavier, H.; Nolan, S. P. *Chem. Commun.* **2010**, *46*, 841–861.
- (17) (a) Müller, A.; Otto, S.; Roodt, A. *Dalton Trans.* **2008**, 650–657. (b) Erre, G.; Enthaler, S.; Junge, K.; Gladiali, S.; Beller, M. *J. Mol. Catal. A: Chem.* **2008**, *280*, 148–155.
- (18) Fleckenstein, C. A.; Plenio, H. *Chem. - Eur. J.* **2007**, *13*, 2701–2716.
- (19) For a recent study on biarylbinopine ligands: Franzoni, I.; Guénee, L.; Mazet, C. *Tetrahedron* **2014**, *70*, 4181–4190.
- (20) Kefalidis, C. E.; Baudoin, O.; Clot, E. *Dalton Trans.* **2010**, *39*, 10528–10535.
- (21) Ackermann, L. *Chem. Rev.* **2011**, *111*, 1315–1345.
- (22) Bruno, N. C.; Tudge, M. T.; Buchwald, S. L. *Chem. Sci.* **2013**, *4*, 916–920.
- (23) Harada, N. *Chirality* **2008**, *20*, 691–723.
- (24) The absolute configurations of products in our preliminary communication were later found to be misassigned. The original paper was corrected accordingly.
- (25) (a) Motti, E.; Catellani, M. *Adv. Synth. Catal.* **2008**, *350*, 565–569. (b) Bheeter, C. B.; Jin, R.; Bera, J. K.; Dixneuf, P. H.; Doucet, H. *Adv. Synth. Catal.* **2014**, *356*, 119–124.
- (26) Gordon, H. L.; Freeman, S.; Hudlicky, T. *Synlett* **2005**, 2911–2914.
- (27) Figg, T. M.; Wasa, M.; Yu, J.-Q.; Musaev, D. G. *J. Am. Chem. Soc.* **2013**, *135*, 14206–14214.
- (28) For the intermolecular proton abstraction mechanism with bidentate phosphines: Pascual, S.; de Mendoza, P.; Braga, A. A. C.; Maseras, F.; Echavarren, A. M. *Tetrahedron* **2008**, *64*, 6021–6029.
- (29) Alternatively, the corresponding *in situ* generated diphosphine mono-oxide could be responsible for this behavior.
- (30) For a positive nonlinear effect observed with binopine ligands in Rh-catalyzed asymmetric hydrogenation involving RhL<sub>2</sub> species: Enthaler, S.; Erre, G.; Junge, K.; Holz, J.; Börner, A.; Alberico, E.; Nieddu, I.; Gladiali, S.; Beller, M. *Org. Process Res. Dev.* **2007**, *11*, 568–577.
- (31) Satyanarayana, T.; Abraham, S.; Kagan, H. B. *Angew. Chem., Int. Ed.* **2009**, *48*, 456–494.
- (32) Boutadla, Y.; Davies, D. L.; Macgregor, S. A.; Poblador-Bahamonde, A. I. *Dalton Trans.* **2009**, 5820–5831.
- (33) Ligand **1a** was chosen for this study due to the symmetrical character of the *t*-Bu group which greatly simplified conformational issues.
- (34) Adamo, C.; Barone, V. *J. Chem. Phys.* **1999**, *110*, 6158–6170.
- (35) (a) Grimme, S.; Ehrlich, S.; Goerigk, L. *J. Comput. Chem.* **2011**, *32*, 1456–1465. (b) Grimme, S.; Antony, J.; Ehrlich, S.; Krieg, H. *J. Chem. Phys.* **2010**, *132*, 154104–154119.
- (36) Marenich, A. V.; Cramer, C. J.; Truhlar, D. G. *J. Phys. Chem. B* **2009**, *113*, 6378–6396.
- (37) The transition state structures with the phosphine ligand coordinated *cis* to the Pd–C(sp<sup>2</sup>) bond were also considered. The most stable TS was *cis*-S-S, with *cis*-R-S, *cis*-R-R, and *cis*-S-R lying at 1.6, 4.1, and 4.6 kcal mol<sup>-1</sup> higher in energy, respectively. These results completely fail to reproduce the diastereoisomeric and enantiomeric ratio observed experimentally.